Available online at www.sciencedirect.com
SCIENCE DIRECT®
Carbohydrate Research 340 (2005) 2654–2660
Carbohydrate RESEARCH

Molecular mobility and the glass transition in amorphous glucose, maltose, and maltotriose

Sonali Shirke and Richard D. Ludescher*

Department of Food Science, Rutgers, The State University of New Jersey, 65 Dudley Road, New Brunswick, NJ 08901-8520, USA

Received 19 May 2005; accepted 10 August 2005
Available online 22 September 2005

Abstract—We have used measurements of the phosphorescence intensity decay of the triplet probe erythrosin B, dispersed in amorphous glucose, maltose, and maltotriose at probe:sugar mole ratios of $\sim$1:10^4, to monitor the molecular mobility of the sugar matrix in the glass and melt around the glass-transition temperature (T_g). Intensity decays were well fit using a stretched-exponential decay model in which the Kohlrausch–Williams–Watts lifetime τ and the stretching exponent β are the physically meaningful parameters. When normalized to the glass-transition temperature, the erythrosin lifetime decreased in the order glucose > maltose > maltotriose. Analysis of the lifetime provided an estimate of the collisional quenching constant for deexcitation of the triplet state (k_{TS0}); k_{TS0} increased in the order glucose < maltose < maltotriose over the range of T–T_g from about −40 to 50 °C. Although approximately constant in the glass, the magnitude of β decreased around T_g in the order glucose > maltose > maltotriose, indicating that the lifetime heterogeneity increased in the order glucose < maltose < maltotriose. These data demonstrate that both the average rate of matrix molecular mobility and the width of the distribution of matrix mobility rates around the glass transition increase with an increase in the molecular size of the sugar in this homologous series.

Keywords: Molecular mobility; Glass transition; Phosphorescence; Triplet state lifetime; Amorphous sugar; Glucose; Maltose; Maltotriose

1. Introduction

The propensity of sugars and other carbohydrates to vitrify from the melt or from concentrated aqueous solution plays a significant role in phenomena as diverse as the worldwide confection industry,[1] the stability of dried and frozen foods,[2–4] and the desiccation tolerance of spores, seeds, and even whole organisms.[5–8] Glass formation upon cooling or dehydration follows a dramatic, even spectacular decrease in viscosity due to comparable decreases in the underlying rates of translational as well as rotational and segmental mobility.[9] Although much effort has been expended in determining the temperature at which the amorphous material undergoes the transition from a flowable liquid or malleable rubber to a rigid, brittle glass, a full physical picture of the vitreous state requires more detailed studies of the effect of temperature and composition on the rates and extents of specific modes of matrix mobility, either internal modes of segmental mobility of individual molecules or external modes of matrix relaxation due to collective motions of groups of molecules.

A variety of physical techniques including dielectric and mechanical relaxation,[10–12] and NMR,[13,14] EPR,[15] and phosphorescence[16–18] spectroscopy have been used to characterize the molecular mobility of amorphous sugars and carbohydrates. The phosphorescence intensity decay of erythrosin B (tetraiodofluorescein) embedded in amorphous sugars has recently been shown to be sensitive to the molecular mobility in the glassy state and changes in mobility at the glass transition.[19–21] We report here the mobility measurements based on analysis of the temperature dependence of the erythrosin emission lifetime in amorphous thin films of the

* Corresponding author. Tel.: +1 732 932 9611x231; fax: +1 732 932 6776; e-mail: ludescher@aesop.rutgers.edu

0008-6215/$ - see front matter © 2005 Elsevier Ltd. All rights reserved.
doi:10.1016/j.carres.2005.08.016

homologous series glucose, maltose, and maltotriose. These data indicate that the matrix molecular mobility varies in the order glucose < maltose < maltrotriose in the region from ~40 °C below to ~40 °C above the glass-transition temperature (T_g), indicating that the molecular mobility is actually higher in sugars with higher molecular weights and thus higher glass-transition temperatures.

2. Results

Phosphorescence intensity decays from erythrosin B (tetraiodofluorescein) dispersed at dye:sugar mole ratios of ~1:10^4 in amorphous glucose, maltose, and maltotriose are plotted in Figure 1. These decay transients were well fit using a stretched-exponential decay model (Eq. 1) in which the Kohlrausch–Williams–Watts lifetime τ

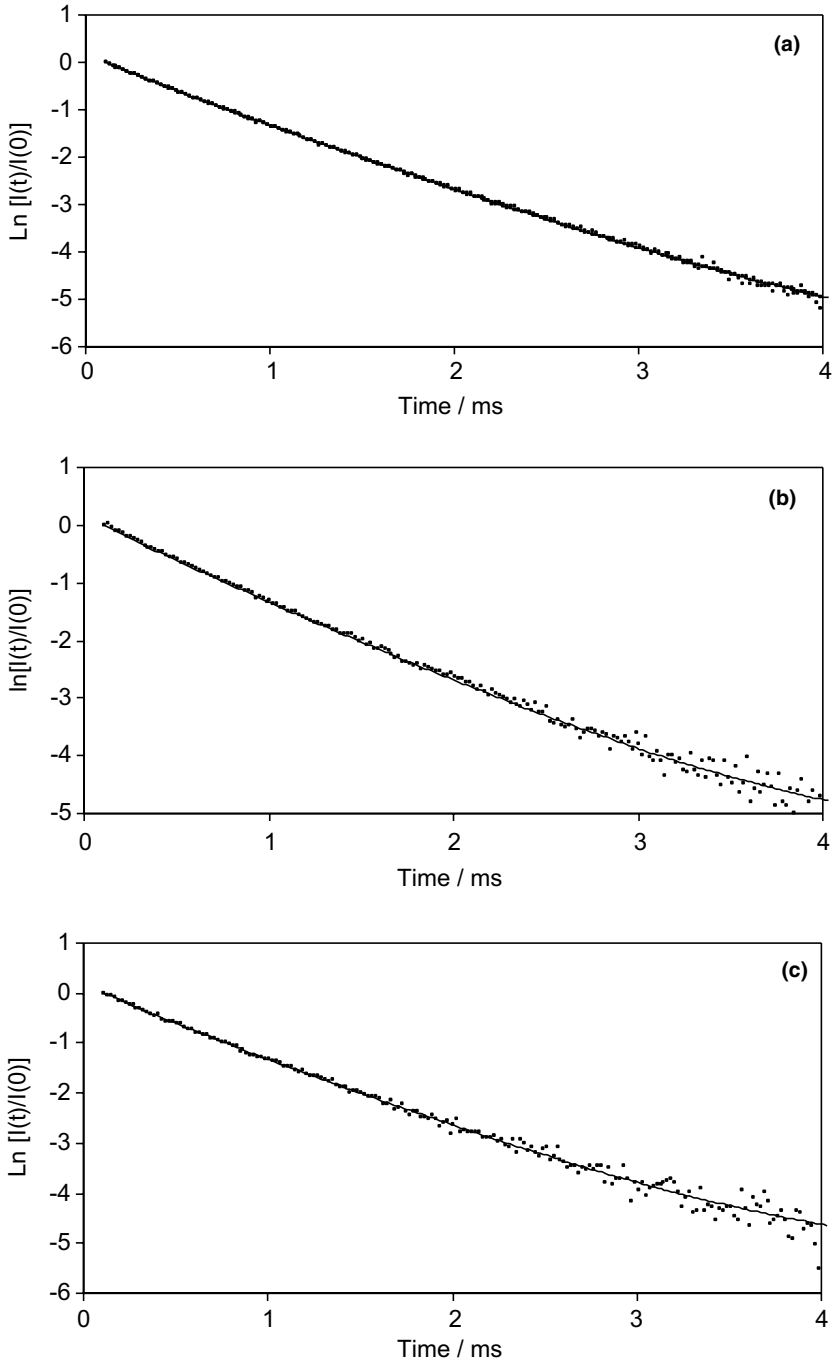

Figure 1. Phosphorescence intensity decays from erythrosin B dispersed in amorphous glucose at 0 °C (a), maltose at −25 °C (b), and maltotriose at 20 °C (c). Continuous curves through the data are stretched-exponential model fits (Eq. 1) using the following values for τ and β, respectively: 0.627 ms and 0.922 for glucose; 0.625 ms and 0.927 for maltose; and 0.630 ms and 0.922 for maltotriose.

and the stretching exponent β are the physically relevant parameters.[22,23] The fit lifetimes and stretching exponents for decays collected over the temperature range from −25 to 150 °C are plotted in Figure 2 versus T–T_g for each sugar to highlight the effect of the glass transition on these physical parameters.

The phosphorescence lifetimes in all three sugars ranged from a maximum of ~0.65 ms in the glassy state to a minimum of ~0.05–0.1 ms in the melt above T_g. The temperature interval over which the lifetime decreased through this range, however, differed dramatically in the three sugars. In glucose, the lifetime decreased only gradually in the glassy state just below T_g and more dramatically in the melt above T_g. In maltotriose, on the other hand, the lifetime decreased significantly in the glassy state well below T_g and less significantly above T_g. The lifetime behavior in maltose was intermediate between these two cases.

The stretching exponent β varied from ~0.95 in the glass at low temperature to ~0.6 in the melt at high temperature in these sugars. The thermal behavior of the stretching exponent also exhibited systematic differences among the sugars. The value of β was essentially constant at 0.90–0.95 in all three sugars in the glass at low temperature. In glucose, β remained constant into the melt, only showing a decrease of about 40 °C above T_g. In maltotriose, on the other hand, β began to decrease in the glass ~25 °C below T_g. The behavior in maltose was intermediate between these two cases.

The lifetime of erythrosin B reflects values of the rate constants for radiative emission k_{RP}, reverse intersystem crossing k_{TS1}, and collisional quenching k_{TS0} (Eq. 2, Section 4).[19,24] The value of k_{RP} is 41 s^{-1} and constant.[24,25] Since the magnitude of k_{TS1} can be estimated,[19] it is possible to calculate k_{TS0} as a function of temperature from Eq. 2. Values for k_P ($= 1/\tau$), estimated values of k_{TS1}, and calculated values for the collisional quenching constant k_{TS0} for erythrosin B in glucose and maltotriose are plotted versus T–T_g in Figure 3; comparable calculations for erythrosin B in maltose are published elsewhere.[21] These calculations indicate that the temperature-induced increases in k_{TS0} had the largest influence on the magnitude of the erythrosin B lifetime.

The value of k_{TS0} as a function of T–T_g for glucose, maltose, and maltotriose is plotted in Figure 4. The magnitude of k_{TS0} was approximately constant at

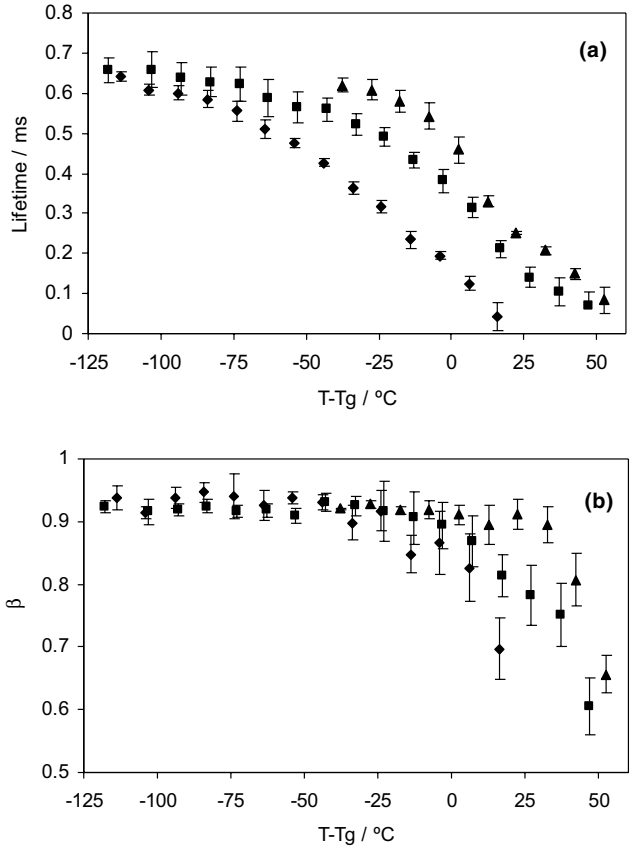

Figure 2. Effect of temperature on the lifetime τ (a) and stretching exponent β (b) for phosphorescence of erythrosin B dispersed in amorphous glucose (▲), maltose (■), and maltotriose (♦). Data plotted versus T–T_g using T_g values of 38, 93, and 134 °C for glucose, maltose, and maltotriose, respectively. Data for erythrosin B in maltose are from Shirke and Ludescher.[21]

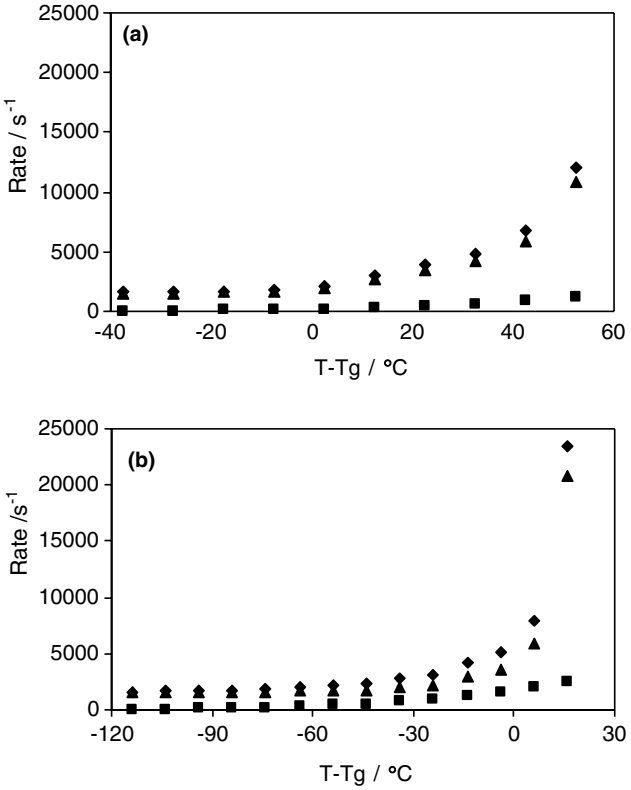

Figure 3. Effect of temperature on the photophysical rate constants k_P (♦), k_{TS1} (■), and k_{TS0} (▲) for erythrosin B phosphorescence in glucose (a) and maltotriose (b). Data plotted versus T–T_g using T_g values of 38 and 134 °C for glucose and maltotriose, respectively.

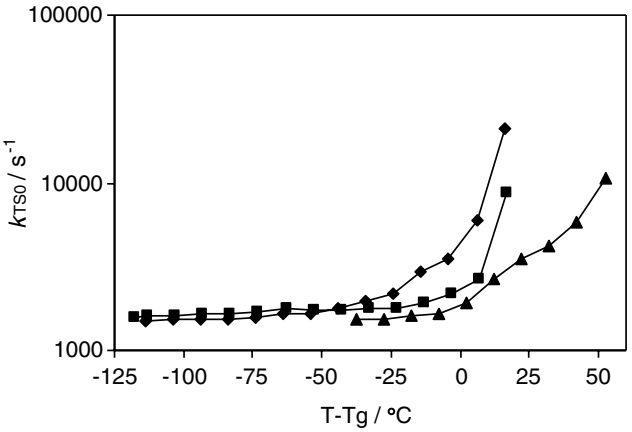

Figure 4. Effect of temperature on the non-radiative decay rate (k_{TS0}) for erythrosin B phosphorescence in amorphous glucose (▲), maltose (■), and maltotriose (♦). Data plotted versus T–T_g using T_g values of 38, 93, and 134 °C for glucose, maltose, and maltotriose, respectively. Data for erythrosin B in maltose are from Shirke and Ludescher.[21]

$\sim$1600 s^{-1} in all three sugars at temperatures well below the glass transition. As suggested by the temperature dependence of the lifetime, however, the collisional quenching constant responded quite differently to temperature in the three sugars. In glucose, k_{TS0} was constant in the glass and only began to increase, albeit gradually, in the melt at T_g and above. In maltotriose, on the other hand, k_{TS0} increased gradually in the glass beginning $\sim$40 °C below T_g and then increased dramatically at the T_g. Again, the behavior in maltose was intermediate between these two cases.

3. Discussion

We have used phosphorescence intensity decay data from erythrosin B to evaluate how changes in molecular size modulate molecular mobility in amorphous solids of the homologous series glucose, maltose, and maltotriose. As in our previous studies of amorphous sucrose,[19] maltose, and maltitol[21,26] these intensity decays were well fit using a stretched-exponential decay model. Such a model provides two physically relevant parameters, the Kohlrausch–Williams–Watts lifetime τ and the stretching exponent β. The KWW lifetime, which essentially reflects the peak of an asymmetric distribution of lifetimes,[23] provides information about the rate constants for de-excitation of the excited triplet state. The stretching exponent β provides an estimate of the width of the distribution of lifetimes required to fit the intensity decay; values of β near unity indicate a narrow lifetime distribution, which becomes single valued (monoexponential) at $\beta = 1$; as β decreases to zero, the width of the asymmetric distribution increases dramatically.[23] The stretched-exponential decay function is thought to provide an appropriate kinetic model for the description of rate processes in hierarchically structured amorphous materials.[27–33]

Analysis of the temperature dependence of the lifetime indicates that the rate constant for intersystem crossing to the ground state (k_{TS0}) is sensitive to the physical state of the amorphous matrix. The magnitude of k_{TS0}, the collisional quenching constant, is sensitive to internal factors related to vibrational coupling between the excited T_1 state and the S_0 ground state[34] as well as external factors related to dissipation of the vibrational energy of the excited probe into the surrounding matrix.[35] Since the efficiency of this vibrational coupling is related to the overall mobility of the matrix,[36] the magnitude of k_{TS0} provides a direct measure of matrix mobility.[19,21]

Matrix mobility increases with molecular size in both the glass and melt in these sugars. Even when scaled to T_g, k_{TS0} increased in the order glucose < maltose < maltotriose at all temperatures ranging from $\sim$40 °C below T_g to $\sim$50 °C above T_g. This correlation of matrix mobility with molecular size (and thus T_g) is consistent with FTIR studies by Wolkers and co-workers, indicating that the vibrational frequency of the OH stretch (ν_{OH}) and the wavenumber temperature coefficient (WTC) for the OH stretch, the slope of the ν_{OH} versus temperature plot, increase with increasing molecular weight in amorphous sugars.[37,38] The FTIR data thus indicate that the hydrogen-bond length increases (ν_{OH} increases) and the hydrogen-bond strength decreases (WTC increases) with increasing sugar molecular weight.[39] Since the sugar matrix is primarily held together by a random network of hydrogen bonds, a matrix with longer and weaker bonds might be expected to exhibit higher rates of matrix molecular mobility. Direct measurements of probe rotational mobility using EPR[15,40] also indicate that spin probes have shorter rotational correlation times, and thus faster rotational mobility, in sugars of higher molecular weight.

Ionic conductivity, and consequently the translational mobility of K and Cl ions, was also found to vary in the order maltotriose > maltose > glucose in amorphous supercooled mixtures of carbohydrates with KCl and water near the glass transition.[48] Ionic mobility scales with viscosity, and thus with the main structural relaxation in liquids. Although the conductivity in supercooled carbohydrate solutions was much higher (10^4- to 10^8-fold) than that expected based on the matrix viscosity, indicating that the ionic mobility is not intimately coupled to the matrix mobility, it is probable that ion mobility and phosphorescence quenching reflect the same underlying variations in matrix mobility.

It is also significant that the shapes of the $k_{TS0}(T)$ curves differ for each sugar; it was not possible to find any scaling temperature that superimposes these curves. Temperature thus appeared to have a distinctly different effect on the matrix mobility of each sugar. Such

behavior is consistent with differences in the length and strength of the hydrogen-bond network among sugars of different molecular weight.

It is also interesting to note that the dispersion of lifetimes followed a similar trend as the mobility. The erythrosin decays are characterized by β values of 0.9–0.95 in the glass state up to about 20 °C below T_g for all three sugars. At temperatures near T_g, however, β began to decrease, first in maltotriose at T–$T_g \approx -20$ °C, then in maltose at $\sim T_g$, and finally in glucose only at T–$T_g \approx +40$ °C. Since the dispersion in lifetimes reflects a dispersion in the underlying photophysical rate constants, this behavior indicates that the systematic increase in k_{TS0} around T_g in these sugars was accompanied by a systematic increase in the width of the distribution of k_{TS0} values. Thus, not only the rate of matrix mobility increased with molecular size, but also the width of the distribution of rates increased with molecular size: sugars of higher molecular weight were both more mobile and more dynamically heterogeneous.

In summary, the collisional quenching rates calculated from intensity decays of erythrosin B phosphorescence provide direct evidence for differences in the matrix molecular mobility in amorphous glucose, maltose, and maltotriose. These differences clearly indicate that the matrix molecular mobility, as well as heterogeneity in the matrix mobility, increases with molecular weight in this homologous series of sugars. The failure of the collisional quenching constant to scale directly with T_g indicates that mobility is more constrained in a matrix made of smaller sugar molecules. Such behavior is consistent with FTIR studies, indicating that there are systematic differences in the length and strength of the hydrogen-bond network in amorphous sugars such that the length increases and the strength decreases with an increase in sugar molecular weight.

4. Experimental

4.1. Sample preparation

Glucose, maltose, and maltotriose were purchased from Sigma–Aldrich (St. Louis, MO) with minimum purity of 98% and were used without further purification. These components were dissolved to near saturation in deionized water at room temperature. The free acid form of erythrosin B (Ery B) was dissolved in spectrophotometer grade *N*,*N*-dimethylformamide (DMF) to make a 10 mM solution; an aliquot from this solution was added to each of the sugar and sugar alcohol solutions to obtain a solution with dye:sugar molar ratio of $\sim 1{:}10^4$. An aliquot (15 μL) of the dye-containing sugar solutions was spread on a quartz slide 3 cm × 1.35 cm (NSG Precision Cells, Hicksville, NY) and then dried for 5 min under a 1600 W hairdryer (Vidal Sassoon, NY). The final thickness of the films was in the range of 10–40 μm as measured by micrometer (Mitutoyo Corp., Japan). The slides were stored in a desiccator containing P_2O_5 and Drierite for at least 4 days prior to luminescence measurements. The slides were checked for crystallization under crossed polarizers using a Nikon Type 102 dissecting microscope (Nikon, Inc., Japan). Glass-transition temperatures were determined by averaging values from the literature; T_g was 38 °C for glucose,[41] 93 °C for maltose,[42–45] and 134 °C for maltotriose.[46]

4.2. Luminescence measurements and analysis

All luminescence measurements were made on a Cary Eclipse Fluorescence Spectrophotometer (Varian Instruments, Walnut Creek, CA). A slide was fitted diagonally into a standard fluorescence cuvette, which was flushed with oxygen-free N_2 gas for at least 15 min prior to measurements. The temperature was controlled using a TLC 50 thermoelectric heating/cooling system (Quantum Northwest, Spokane, WA). For measurements below room temperature, the chamber surrounding the cuvette holder was flushed with dry air to eliminate moisture condensation.

Intensity decays used excitation at 530 nm (bandwidth 20 nm) and emission collected at 680 nm (bandwidth 20 nm); decays were collected over the temperature range from 0 to 90 °C for glucose, from −25 to 140 °C for maltose, and from −25 to 150 °C for maltotriose. Samples were equilibrated for 5 min at each temperature before collecting data. The intensity was collected as a function of time following the lamp flash over a window of 4 ms following a delay time of 0.1 ms and using a gate time of 0.02 ms; 10 cycles were summed to generate each decay transient. The intensity transients were analyzed using a stretch-exponential decay function:[19,47]

$$I(t) = I(0)\exp[-(t/\tau)^{\beta}] + \text{constant} \qquad (1)$$

where $I(0)$ is the initial intensity at time zero, τ is the Kohlrausch–Williams–Watts lifetime[22] and β is the stretching exponent,[23] a parameter that varies from 0 to 1. The appropriateness of this decay model for erythrosin B phosphorescence intensity decays in amorphous solids is discussed at length elsewhere.[19,47] Data analyses used the program NFIT (Island Products, Galveston, TX), which uses a non-linear least squares algorithm that varies the adjustable parameters to minimize χ^2. All fits gave R^2 values in the range of 0.99–1.0 and modified residuals ((data − fit)/data$^{1/2}$) plots that varied randomly about zero.

4.3. Photophysical scheme

Our analysis of the photophysics of erythrosin B follows that of Duchowicz et al.,[24] using slightly different nomenclature. The measured emission rate for phosphorescence

($k_P = 1/\tau$) is the sum of all possible deexcitation rates for the triplet state T_1:

$$k_P = k_{RP} + k_{TS0}(T) + k_{TS1}(T) \quad (2)$$

where k_{RP} is the rate of radiative emission to the ground state S_0, k_{TS0} is the rate of intersystem crossing to S_0 (rate of collisional quenching), and k_{TS1} is the rate of reverse intersystem crossing to the excited singlet S_1; only the latter two rate constants vary with temperature. (Oxygen quenching is assumed negligible due to the elimination of oxygen.)

The rate of radiative emission (k_{RP}) is 41 s^{-1} and constant.[24,25] The rate of reverse intersystem crossing to S_1 (k_{TS1}) is a thermally activated process:[24]

$$k_{TS1} = k^0_{TS1} \exp(-\Delta E_{TS}/RT) \quad (3)$$

where k^0_{TS1} is the maximum rate of intersystem crossing from T_1 to S_1 at high temperature, ΔE_{TS} is the energy gap between S_1 and T_1, $R = 8.314$ J K^{-1} mol^{-1}, and T is the temperature in Kelvin. The value of ΔE_{TS} is calculated from the slope of a Van't Hoff plot of the natural logarithm of the ratio of intensity of delayed fluorescence (I_{DF}) to phosphorescence (I_P) ($\ln(I_{DF}/I_P)$ vs $1/T$);[19,24] ΔE_{TS} for erythrosin in maltose is 33 kJ mol^{-1};[21] the same value was used for glucose and maltotriose. The literature values for k^0_{TS1} for erythrosin B vary from 0.3×10^7 s^{-1} in ethanol and 6.5×10^7 s^{-1} in water[24] to 111×10^7 s^{-1} in solid polyvinyl alcohol,[25] and thus provide little guidance. We estimated that $k^0_{TS1} = 3.0 \times 10^7$ s^{-1} for Ery B in maltose[21] and in sucrose;[19] the same value was used for erythrosin B in maltotriose while a value of 6.5×10^7 s^{-1} was used for glucose.[20] Variations in the magnitude of k^0_{TS1} over this range do not affect the conclusions of this study.

Acknowledgments

The author, R.D.L., thanks Dr. Ann Oliver for first bringing the studies relating to sugar molecular mobility and sugar molecular weight to his attention. This research was supported by a grant (# 2001-01683) from the National Research Initiative of the US Department of Agriculture.

References

1. Edwards, W. P. *The Science of Sugar Confectionery*; Royal Society of Chemistry: Cambridge, 2000.
2. Roos, Y. *Phase Transitions in Foods*; Academic Press: San Diego, CA, 1995.
3. Fennema, O. Water and Ice. In *Food Chemistry*; Fennema, O., Ed., 3rd ed.; Marcel Dekker: NY, 1996; pp 17–94.
4. Le Meste, M.; Champion, D.; Roudaut, G.; Blond, G.; Simatos, D. *J. Food Sci.* **2002**, *67*, 2444–2458.
5. Crowe, J. H.; Carpenter, J. F.; Crowe, L. M. *Ann. Rev. Physiol.* **1998**, *60*, 73–103.
6. Crowe, J. H.; Oliver, A. E.; Tablin, F. *Integrat. Comp. Biol.* **2002**, *42*, 497–503.
7. Tunnacliffe, A.; Lapinski, J. *Trans. Roy. Soc. Lond. Ser. B: Biol. Sci.* **2003**, *358*, 1755–1771.
8. Buitink, J.; Leprince, O. *Cryobiology* **2004**, *48*, 215–228.
9. Zallen, R. *The Physics of Amorphous Solids*; John Wiley & Sons: New York, 1983.
10. Chan, R. K.; Pathmanathan, K.; Johari, G. P. *J. Phys. Chem.* **1986**, *90*, 6358–6362.
11. Noel, T. R.; Ring, S. G.; Whittam, M. A. *J. Phys. Chem.* **1992**, *96*, 5662–5667.
12. Faivre, A.; Niquet, G.; Maglione, M.; Fornazero, J.; Jal, J. F.; David, L. *Eur. Phys. J. B* **1999**, *10*, 277–286.
13. van den Dries, I. J.; van Dusschoten, D.; Hemminga, M. A. *J. Phys. Chem. B* **1998**, *102*, 10483–10489.
14. Moran, G. R.; Jeffrey, K. R. *J. Chem. Phys.* **1999**, *110*, 3472–3483.
15. Buitink, J.; Van den Dries, I. J.; Hoekstra, F. A.; Alberda, M.; Hemminga, M. A. *Biophys. J.* **2000**, *79*, 1119–1128.
16. Wagner, H.; Richert, R. *J. Non-Cryst. Solids* **1998**, *242*, 19–24.
17. Wagner, H.; Richert, R. *J. Phys. Chem. B* **1999**, *103*, 4071–4077.
18. Richert, R. *Europhys. Lett.* **2001**, *54*, 767–773.
19. Pravinata, L. C.; You, Y.; Ludescher, R. D. *Biophys. J.* **2005**, *88*, 3551–3561.
20. Shirke, S. M.S. Thesis, Rutgers University, New Brunswick, NJ, 2005.
21. Shirke, S.; Ludescher, R. D. *J. Phys. Chem. B* **2005**, *109*, 16119–16126.
22. Williams, G.; Watts, D. C. *Trans. Faraday Soc.* **1970**, *66*, 80–85.
23. Lindsey, C. P.; Patterson, G. D. *J. Chem. Phys.* **1980**, *73*, 3348–3357.
24. Duchowicz, R.; Ferrer, M. L.; Acuna, A. U. *Photochem. Photobiol.* **1998**, *68*, 494–501.
25. Lettinga, M. P.; Zuilhof, H.; van Zandvoort, A. M. J. *Phys. Chem. Chem. Phys.* **2000**, *2*, 3697–3707.
26. Shirke, S.; Ludescher, R. D. *Carbohydr. Res.* **2005**, *340*, in this issue, please see doi:10.1016/j.carres.2005.08.015.
27. Hofstraat, J. W.; Verhey, H. J.; Verhoeven, J. W.; Kumke, M. U.; McGown, L. B.; Novikov, E. G.; van Hoek, A.; Visser, A. J. W. G. *Proc. SPIE* **1996**, *2705*, 110–121.
28. Richert, R. *J. Phys. Chem. B* **1997**, *101*, 6323–6326.
29. Richert, R. *J. Non-Cryst. Solids* **1998**, *235–237*, 41–47.
30. Richert, R. *J. Chem. Phys.* **2000**, *113*, 8404–8429.
31. Linnros, J.; Lalic, N.; Galeckas, A.; Grivickas, V. *J. Appl. Phys.* **1999**, *86*, 6128–6134.
32. Jaba, N.; Kanoun, A.; Mejri, H.; Maaref, H.; Brenier, A. *J. Phys.: Condens. Matter* **2000**, *12*, 7303–7309.
33. Pophristic, M.; Lukacs, S. J.; Long, F. H.; Tran, C. A.; Ferguson, I. T. *Proc. SPIE* **2000**, *3938*, 105–112.
34. Papp, S.; Vanderkooi, J. M. *Photochem. Photobiol.* **1989**, *49*, 775–784.
35. Fischer, C. J.; Gafni, A.; Steele, D. G.; Schauerte, J. A. *J. Am. Chem. Soc.* **2002**, *124*, 10359–10366.
36. Strambini, G. B.; Gonnelli, M. *Chem. Phys. Lett.* **1985**, *115*, 196–200.
37. Wolkers, W. F.; Oldenhof, H.; Alberda, M.; Hoekstra, F. A. *Biochim. Biophys. Acta* **1998**, *1379*, 83–96.
38. Wolkers, W. F.; Oliver, A. E.; Tablin, F.; Crowe, J. H. *Carbohydr. Res.* **2004**, *339*, 1077–1085.
39. Jeffrey, G. A. *An Introduction to Hydrogen Bonding*; Oxford University Press: NY and Oxford, 1997.
40. Dzuba, S. A.; Golovina, Y. A.; Tsvetkov, Y. D. *J. Magn. Reson., Ser B* **1993**, *101*, 134–138.
41. Noel, T. R.; Parker, R.; Ring, S. G. *Carbohydr. Res.* **2000**, *329*, 839–845.
42. Roos, Y. H. *Carbohydr. Res.* **1993**, *238*, 39–48.

43. Orford, P. D.; Parker, R.; Ring, S. G. *Carbohydr. Res.* **1990**, *196*, 11–18.
44. Noel, T. R.; Parker, R.; Ring, S. G. *Carbohydr. Res.* **1996**, *282*, 193–206.
45. Noel, T. R.; Parker, R.; Ring, S. M.; Ring, S. G. *Carbohydr. Res.* **1999**, *319*, 166–171.
46. Orford, P. D.; Parker, R.; Ring, S. G.; Smith, A. C. *Int. J. Biol. Macromol.* **1989**, *11*, 91–96.
47. Simon-Lukasik, K. V.; Ludescher, R. D. *Food Hydrocolloids* **2005**, *18*, 621–630.
48. Noel, T. R.; Parker, R.; Ring, S. G. *Carbohydr. Res.* **2003**, *338*, 433–438.